Analysis of the Loss Distribution of a 6 kW two Stage Power Supply for 600 V DC Applications

Lukas Fräger[1], Sascha Langfermann[1], Michael Owzareck[1], Dennis Kampen[1], Jens Friebe[2]
[1]BLOCK TRANSFORMATOREN-ELEKTRONIK GmbH
[2]Leibniz Universität Hannover, Institute for Drive Systems and Power Electronics
[1]Max-Planck-Straße 36-46 / [2]Welfengarten 1
[1]Verden / [2]Hannover, Germany
Tel.: +49 / (0) 4231 678 434
Fax: +49 / (0) 4231 678 277
E-Mail: lukas.fraeger@block.eu
URL: http://www.block.eu

Acknowledgements

Parts of this work were funded by the German Federal Ministry for Economic Affairs and Energy (BMWi) under grant number 03EN2010A-G in the project STIM. The authors are responsible for the content of this publication.

Keywords

Voltage Source Inverters (VSI), Modelling, Silicon Carbide (SiC), High frequency power converter, Switching Losses

Abstract

This paper presents a two-stage AC/DC power supply consisting of a silicon carbide power semiconductor based active front end and a dual active bridge DC/DC converter. The paper presents the design considerations, efficiency and loss analysis based on measurements. The focus is specially drawn to the influence of the variable DC-link voltage on the overall efficiency and loss distribution among the two stages.

1 Introduction

Current developments in industry and society lead to the need for high power AC/DC power supplies in low voltage grids (e.g. charging stations, energy storages, DC-grids for industry [1] [2] [3]). Additionally, for future applications, bidirectional supplies are favored to feed power back to the grid (e.g. braking energy, integration of renewables and batteries). This paper presents a $6\ kW$ power supply designed for high power density and good efficiency. It gives a basis for optimization of the efficiency depending on input and output voltage and includes detailed measurement results.

2 System Specification

The power supply is designed to supply a fixed DC voltage of $600\ V$. This voltage can be used to supply off-the-shelf industry inverters that currently work with an uncontrolled rectified DC-link voltage which is at $563\ V$ in a $400\ V$ grid. For worldwide applicability, the power supply must be able to work in most low voltage grids. An overview of worldwide grid voltages is given in Table 1.

Table 1: Excerpt of international grid voltages [4]

Country / Region	Three Phase line to line grid voltage(s)
EU	$400\ V$
USA/Canada	$208\ V, 480V\ , 600\ V$ (only Canada)
Japan	$200\ V$
China	$380\ V$

Open DC-Grids as in [5] are one possible application for the presented power supply. Thus, a galvanic isolation is favored especially when the grids are supposed to have an independent earthing concept (e.g. grounded Δ-Grid to mid point grounded DC-Grid). Also, when connecting multiple supplies in parallel, an isolation can help reducing circular currents between the converters. The resulting specifications are given in Table 2.

Table 2: Specification of AC/DC-power supply

Specified Value	Value
Input voltage range (line to line)	$200\ V$ ... $480\ V$
Output voltage (DC)	$600\ V$ ($550\ V$ ... $650\ V$)
Power	$6\ kW$
Isolation type	*Reinforced*

3 System description and design considerations

A block diagram of the built-up system is given in Figure 1. The system consists of two stages: A bidirectional active front end (AFE) and a bidirectional, galvanically isolated DC/DC converter.

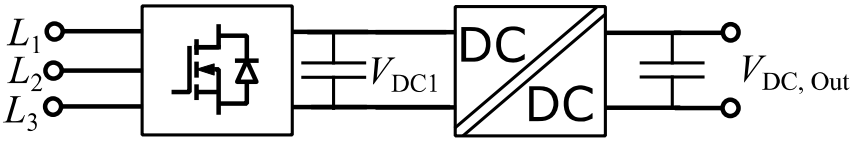

Figure 1: Block diagram of a two stage AC/DC power supply with a three phase input (L_1, L_2, L_3) and DC output ($V_{DC,Out}$)

3.1 Topology Considerations

Both, the AFE as well as the DC/DC converter must provide bidirectional power flow. Due to the recent developments in wide bandgap technologies, efficient converters can be built with SiC MOSFETs in a standard two-level topology.

For the AFE, a three leg, two stage inverter with an integrated All-Pole-LC filter is used. Due to the use of high switching frequencies ($\sim 100\ kHz$), it is possible to reduce the size of the LC filter compared to standard AFEs and integrate it in one housing with the AFE [6]. The specified values for the AFE are shown in Table 3. The losses of the AFE mainly depend on the DC-Link voltage (switching and AC-filter losses) and input current (switching and conduction losses) [7]. The highest losses thus appear for low input voltage (following high input currents) and high DC-Link voltage. While the input current in a certain grid for an intended power is fixed, the DC-Link voltage may be varied. For the bidirectional AFE, it is favorable to be operated close to the minimum DC-Link voltage which can be calculated with the line-to-line voltage $V_{AC,ll}$ and the control reserve factor $R_{C,\%}$ when neglecting the voltage drop across the inductor:

$$V_{DC1,min} = V_{AC,ll} \cdot \sqrt{2} \cdot (1 + R_{C,\%})$$

Table 3: Specification of bidirectional active rectifier

Specified Value	Value
Input voltage range (line to line)	$200\ V \ldots 480\ V$
DC-Link voltage range	$300\ V \ldots 750\ V$

The specification of the DC/DC stage is shown in Table 4. Many different DC/DC converter topologies have been published in recent years [8] [9] [10]. However, for resonant topologies in higher power applications ($> 2\ kW$), expensive capacitors are needed in addition to the transformer. Also, resonant topologies tend to have a limited bidirectional capability in terms of transfer ratio: In one direction, most resonant topologies have a maximum transfer-ratio equal to the transformer ratio. Thus, operated at a high AC input voltage $V_{AC,ll}$, energy transfer to the grid may not be possible at $V_{DC,Out} < V_{DC1,min}$ e.g.

600 V output voltage. To provide full bidirectionality, be able to vary the DC-Link voltage and to lower component cost, a dual active bridge (DAB) is chosen for the DC/DC converter. For first evaluations, the turns ratio of the medium frequency transformer is chosen to be 1:1. However, results show that depending on the preferred grids, a better optimum may be found [8].

Table 4: Specification of DCDC converter

Specified Value	Value
Input voltage range	300 V ... 750 V
Output voltage	600 V
Power	6 kW
Power flow	*Bidirectional*
Isolation	*Reinforced*

3.2 System Description

A resulting overview schematic is given in Figure 2. All power semiconductors are Silicon Carbide MOSFETs, which allow a high switching frequency as well as a high efficiency. All half bridges are 2-level configurations to keep the component count and cost low.

To comply with electromagnetic compatibility (EMC) standards, a grid filter in front of the AFE is needed. The grid filter is integrated with the AFE. On one hand this way the power density can be optimized. Also, current paths for the filter currents are reduced, which reduces EMC issues.

The input and output stage of the DAB converter is comprised of full bridges to utilize the full voltage range at the input and output stage and thus reduce the currents. Also, this configuration enables the use of the third level and thus advanced modulation strategies [11] [12] [13].

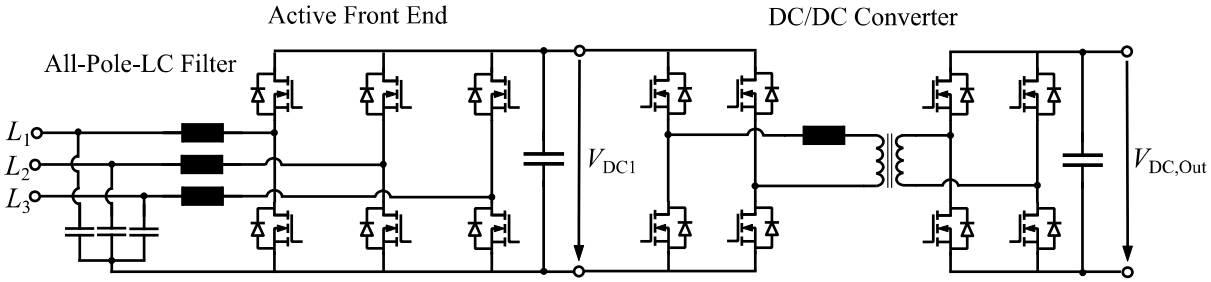

Figure 2: Schematic overview of the presented Power Supply with integrated all-pole-LC-filter, bidirectional AFE and DC/DC converter.

4 Hardware description

The test hardware is shown in Figure 3. For testing purposes, AFE and DC-DC converter are built up separately. However, they are designed to be integrated in a single housing.

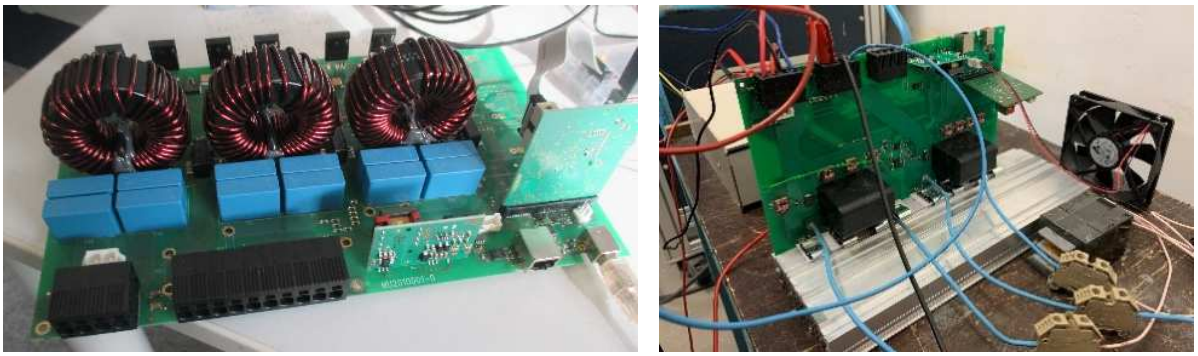

Figure 3: Built up test hardware. Left: AFE with integrated LC filter and right: DC/DC converter with attached MF-Transformer.

Both AFE as well as DC/DC converter are built up with SiC power semiconductors. Lists of relevant components of the AFE and DC/DC converter are given in Table 5 and Table 6 respectively.

Table 5: AFE: List of relevant components and control settings

Component	Type
Semiconductors	Infineon IMZ120R060
DC-Link Capacitor	2x Vishay MKP1848C, 900 V 50 µF
Core Material	Sendust 60µ
Core Size	62x33x25 (Ring Core)
Number of Turns	35
Switching frequency	100 kHz

Table 6: DC/DC converter: List of relevant components and control settings

Component	Type
Semiconductors	Infineon IMZ120R090
DC-Link Capacitor	4x Vishay MKP1848C, 900 V 50 µF (2x primary, 2x secondary)
Core Material	EPCOS N87
Core Size	Stacked 3x EE55/25
Number of Turns Primary / Secondary	10 / 10
Litz Wire	1400x0.05 mm
Switching Frequency	100 kHz

5 Measurement Results

The aim of the presented measurements is to give a detailed picture of the influence of the DC-Link voltage V_{DC1} on the losses of both the AFE as well as the DC/DC converter. Thus, overall losses, losses of the DC/DC converter as well as losses of the AFE are measured and presented. Measurements were done separately with AFE and DC/DC converter. For all measurements, the measurement equipment described in Table 7 is used.

Table 7: Measurement Equipment

Equipment	Type
Oscilloscope	Tek MSO Series 4, 500MHz, 12 bit, 6Ch
Current Probe	TCP0030A
Voltage Probe	THDP0200
Power Analyzer	Yokogawa WT1800

The loss measurements include all losses including auxiliary supply losses for driving, control and fans. The auxiliary losses were analyzed independently and found to be below $4\,W$ for both the DC/DC converter as well as the AFE.

5.1 Loss Distribution

First, the losses of the AFE and the DC/DC converter are analyzed independently. Figure 4 shows the losses at 3.2 kW output power and an input voltage $V_{AC,ll} = 208V$, Figure 5 at 6 kW output power and an input voltage $V_{AC,ll} = 400V$. Thermal measurements showed that the output power must be derated at low input voltages. Thus, measurements with nominal power are only shown for $V_{AC,ll} = 400V$.

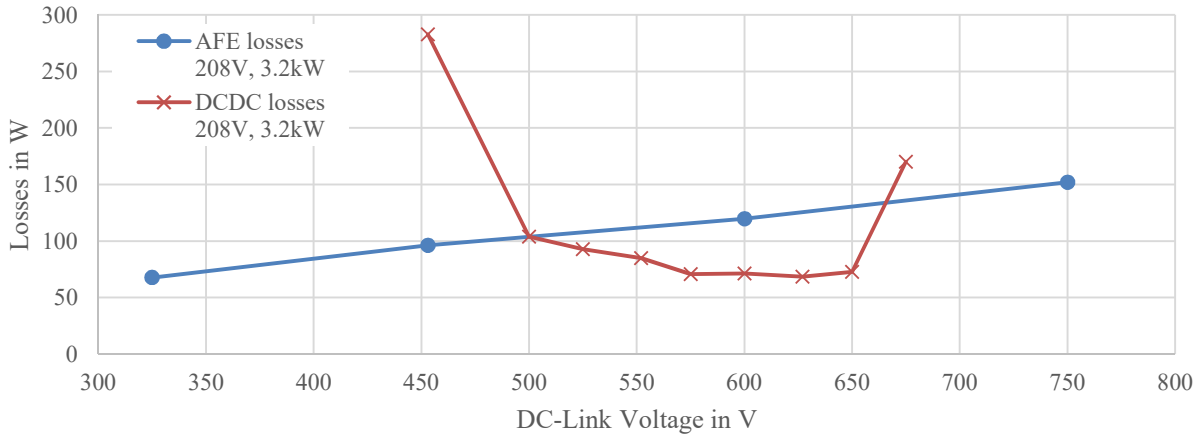

Figure 4: Measured and interpolated losses at 3.2 kW output power, 208 V input voltage and 600V output voltage of the AFE and the DC/DC converter.

Figure 4 shows the loss distribution among DC/DC converter and AFE at $P_{Out} = 3.2\ kW$ and $V_{AC,ll} = 208\ V$ for different DC-link voltages. Clearly, the loss distribution is influenced by the DC-Link voltage: The AFE-losses increase nearly linearly with a higher DC-Link voltage. The DC/DC converter losses increase strongly at transfer ratios far away from 1 (above 1.2 and below 0.9). It is assumed, that the converter leaves the soft switching region here. Between a DC-Link voltage of 500 V and 650 V, the DC/DC converter losses slightly decrease with a rising DC-link voltage. In this region, the losses can be distributed among DC/DC converter and AFE by means of the DC-link voltage. Minimum losses for the AFE can be found at $V_{DC1} = 500\ V$; minimum losses for the DC/DC converter at $V_{DC1} = 625\ V$. Further, for $500V \leq V_{DC1} \leq 650\ V$, the AFE losses dominate due to the low input voltage.

Figure 5 shows the losses of the DC/DC converter and AFE at $P_{Out} = 6\ kW$ and $V_{AC,ll} = 400\ V$ in dependence of the DC-link voltage. The soft switching region is increased compared to the measurements at 3.2 kW. Minimum losses are at $V_{DC1} = 500\ V$ for the DC/DC converter and at $V_{DC1} = 575\ V$ for the AFE respectively. It may be noted, that α and thus the system may operate at $V_{DC1,min} \geq 575\ V$.

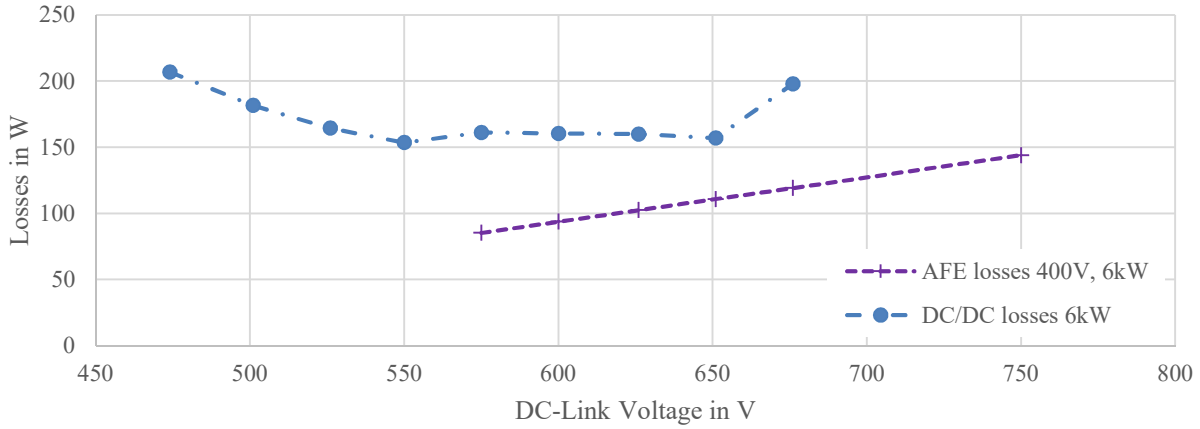

Figure 5: AFE and DC/DC converter losses at 6kW output power and 400V line to line input voltage in dependence on the DC-link voltage.

Figure 6 and Figure 7 show the overall losses for different power and input voltage levels. Figure 6 includes the system losses at $V_{AC,ll} = 208\ V$, Figure 7 at $V_{AC,ll} = 400\ V$.

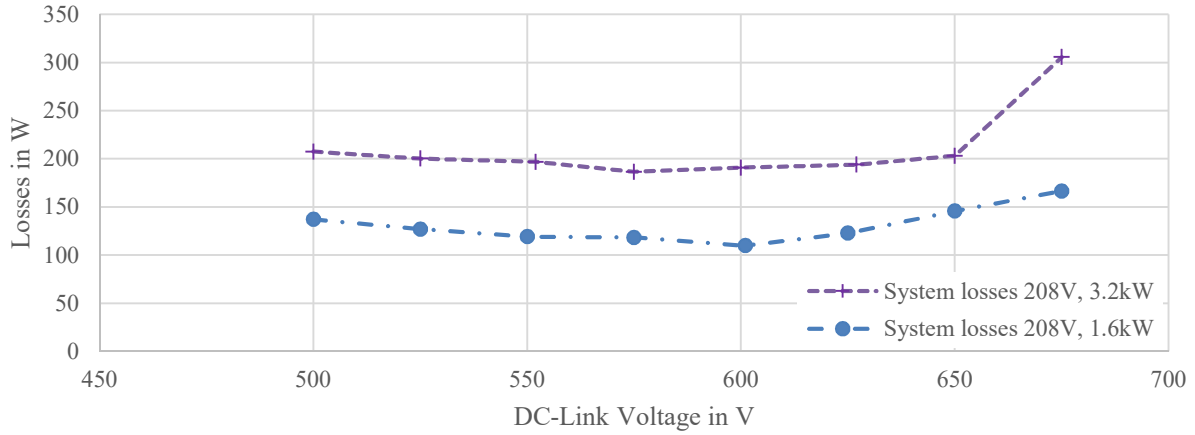

Figure 6: System losses at 208V input voltage, 600V output voltage in dependence of the DC-Link voltage for different output powers.

At $V_{AC,ll} = 208\,V$ the lowest overall losses for 1.6 kW and 3.2 kW are at $V_{DC} = 575\,V$ and $V_{DC1} = 600\,V$ respectively. However, losses of the AFE can be reduced by approximately 15% if operated at $V_{DC1} = 500\,V$ instead. This may be favorable as the AFE losses dominate for low input voltages.

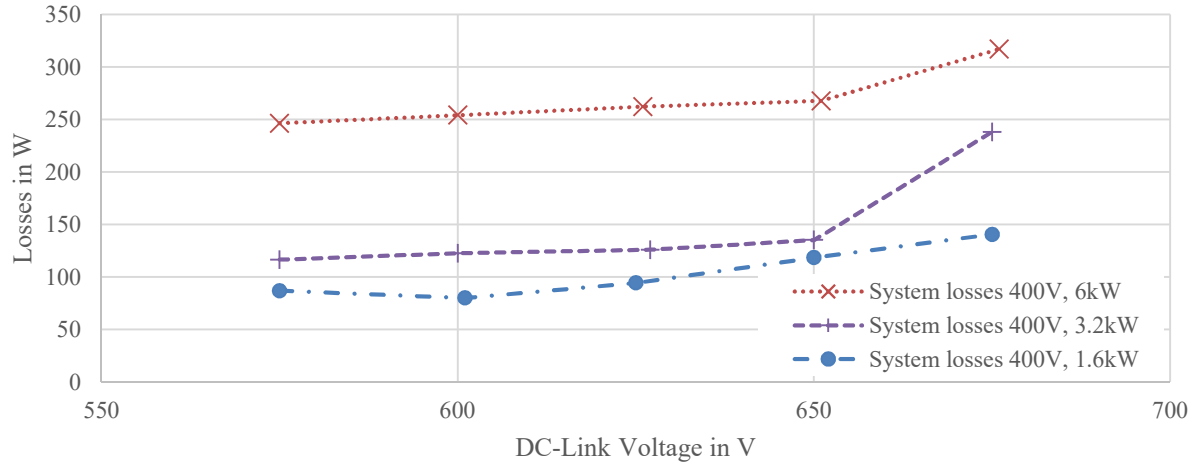

Figure 7: System losses at 400V input voltage, 600V output voltage in dependence of the DC-Link voltage for different output powers.

Figure 7 presents the system losses at $V_{AC,ll} = 400\,V$ at different output powers. At $P_{Out} = 6\,kW$ and $P_{Out} = 3.2\,kW$, the system losses are minimum at $V_{DC1} = V_{DC1,min} = 575\,V$. At $P_{Out} = 1.6\,kW$, losses become minimal at $V_{DC1} = 600\,V$.

At all presented operating points, the DC/DC converter losses would yet be lower for higher DC-link voltages (cmp. Figure 4 and Figure 5). It may be concluded that for the presented operating points a transformer turns ratio smaller than 1:1 would be favorable in terms of system efficiency.

5.2 System Efficiency

To complete the picture of the presented power supply, the overall system efficiency in dependence of the DC-Link voltage V_{DC1} is analyzed. The measurement results are given in Figure 8.

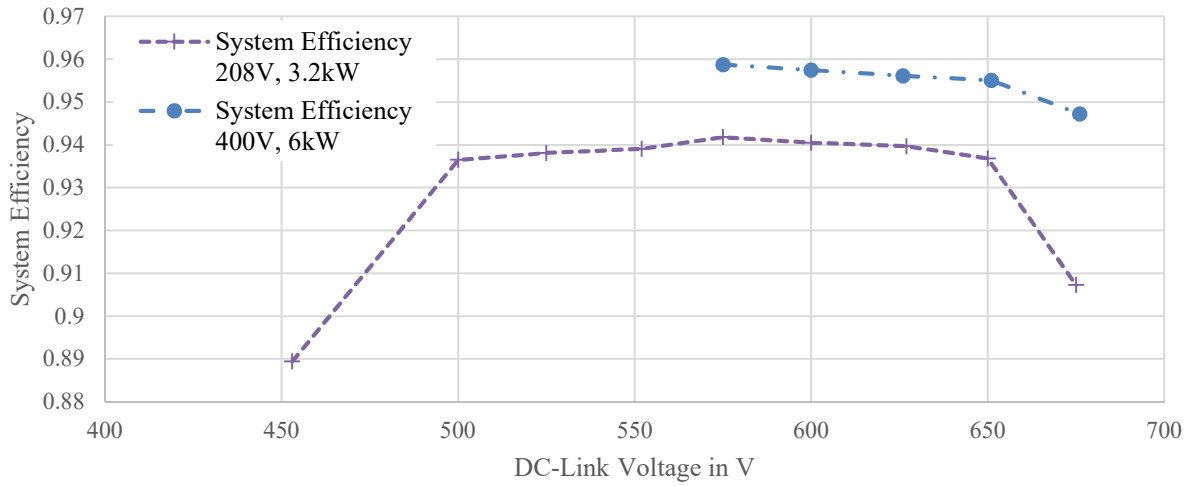

Figure 8: System Efficiency for an output power of 3.2kW and 6kW in dependence of the DC-Link voltage at an input voltage of $V_{AC,ll} = 208$ V and $V_{AC,ll} = 208$ V, respectively, and an output voltage $V_{DC,out} = 600$ V.

Maximum efficiency for both $V_{AC,ll} = 400\ V$ as well as $V_{AC,ll} = 208\ V$ is achieved for a DC-link voltage of $V_{DC1} = 575\ V$. Towards high / low transfer ratios between DC-link and output voltage, the efficiency drops clearly as it leaves the soft switching region of the DAB.

As the AFE-efficiency is much higher at larger input voltages $V_{AC,ll}$, the overall efficiency is higher at an input voltage of $V_{AC,ll} = 400\ V$.

6 Conclusion and Outlook

The paper analyzes the influence of the DC-Link voltage for a specific setup in detail. Results show, that by varying the DC-link voltage, losses can be distributed among the two stages of the AC/DC power supply. Depending on the grid voltage and the output power, different optimum DC-link voltages may be found. In future work, the influence of the DC-Link should be analyzed analytically for general setups. To optimize the DC-link voltage in systems during operation, analytic models are needed to be included in the control of power supplies. Further research should also focus on derating concepts depending on grid/input voltage and output voltage range.

7 References

[1] R. W. D. Doncker, *Fast Charging (350 kW) for Electric Vehicles - Possibilities and Issues,* Eindhoven, 2019.

[2] B. Sattler und S. Wiesner, „Research Project DC-Industrie - Energiewende meets Industrie 4.0," ZVEI - German Electrical and Eletronic Manufacturers' Association, Frankfurt, 2019.

[3] C. Meyer, M. Hoing, A. Peterson und R. W. D. Doncker, „Control and Design of DC-Grids for Offshore Wind Farms," *Conference Record of the 2006 IEEE Industry Applications Conference Forty-First IAS Annual Meeting,* 2006.

[4] "www.worldstandards.eu," 19 12 2021. [Online]. Available: https://www.worldstandards.eu/electricity/three-phase-electric-power/.

[5] B. Sattler and S. Wiesner, "Research Project DC-Industrie - Energiewende meets Industrie 4.0," ZVEI - German Electrical and Eletronic Manufacturers' Association, Frankfurt, 2019.

[6] S. Langfermann, M. Owzareck und L. Fräger, „Design Space Optimization of a SiC Drive Inverter with an Integrated All-Pole Sine Filter," *23rd European Conference on Power Electronics and Applications,* 2021.

[7] L. Fräger, S. Langfermann, M. Owzareck und J. Friebe, „An analytic inverter loss model for design and operation space optimization," *2021 23rd European Conference on Power Electronics and Applications,* 2021.

[8] P. Apte, S. Lin, L. Fräger und J. Friebe, „Design considerations for a 50 kW Dual-Bridge Series Resonant DC/DC Converter with Wide-Inpu Voltage Range for Solid-State Transformers," *2021 IEEE Energy Conversion Congress and Exposition (ECCE),* 2021.

[9] A. Hillers, D. Christen und J. Biela, „Design of a Highly Efficient Bidirectional Isolated LLC," *15th International Power Electronics and Motion Control Conference, EPE-PEMC,* 2012.

[10] B. Zhao, Q. Song, W. Liu und Y. Sun, „Overview of Dual-Active-Bridge Isolated Bidirectional DC–DC Converter for High-Frequency-Link Power-Conversion System," *IEEE Transactions on Power Electronics,* 2014.

[11] A. Jafari, M. S. Nikoo, F. Karakaya and E. Matioli, "Enhanced DAB for Efficiency Preservation Using Adjustable-Tap High-Frequency Transformer".*IEEE Transactions on Power Electronics.*

[12] V. Karthikeyan, S. Rajasekar, S. Pragaspathy und F. Blaabjerg, „A High Efficient DAB Converter under Heavy Load Conditions Using Inner Phase Shift Control," *IEEE International Conference on Power Electronics, Drives and Energy Systems (PEDES),* 2018.

[13] Fräger, Badenhop, Langfermann, Owzareck, Kampen and Friebe, "Dual Active Bridge Converter: Simple Peak Current Limitation by Dual Phase Shift Control," *PCIM 2022,* 2022.

[14] Langmaack et al, „Fast and Universal Semiconductor Loss Calculation Method".*IEEE PEDS 2019.*

[15] D. Christen und J. Biela, „Analytical Switching Loss Modeling Based on Datasheet Parameters for MOSFETs in a Half-Bridge," *IEEE TRANSACTIONS ON POWER ELECTRONICS,* 2019.